Published in final edited form as:

J Am Coll Cardiol. 2016 January 19; 67(2): 174–189. doi:10.1016/j.jacc.2015.10.072.

Metabolic Profiling of Right Ventricular-Pulmonary Vascular Function Reveals Circulating Biomarkers of Pulmonary Hypertension

Gregory D. Lewis, MD[*,†,‡], **Debby Ngo, MD**[†], **Anna R. Hemnes, MD**[§], **Laurie Farrell, RN**[*], **Carly Domos, MS**[*], **Paul P. Pappagianopoulos, MED**[†], **Bishnu P. Dhakal, MD**[*], **Amanda Souza, MS**[‡], **Xu Shi, PHD**[*], **Meredith E. Pugh, MD, MSCI**[§], **Arkadi Beloiartsev, MD**[*], **Sumita Sinha, PHD**[*], **Clary B. Clish, PHD**[‡], and **Robert E. Gerszten, MD**[*,‡,‖]

[*]Cardiology Division, Department of Medicine, Massachusetts General Hospital, Harvard Medical School, Boston, Massachusetts

[†]Pulmonary and Critical Care Unit, Department of Medicine, Massachusetts General Hospital, Harvard Medical School, Boston, Massachusetts

[‡]Broad Institute of MIT and Harvard, Cambridge, Massachusetts

[§]Vanderbilt University Pulmonary Unit, Nashville, Tennessee

[‖]Cardiovascular Research Center, Massachusetts General Hospital, Harvard Medical School, Boston, Massachusetts

Abstract

BACKGROUND—Pulmonary hypertension and associated right ventricular (RV) dysfunction are important determinants of morbidity and mortality, which are optimally characterized by invasive hemodynamic measurements.

OBJECTIVES—This study sought to determine whether metabolite profiling could identify plasma signatures of right ventricular-pulmonary vascular (RV-PV) dysfunction.

METHODS—We measured plasma concentrations of 105 metabolites using targeted mass spectrometry in 71 individuals (discovery cohort) who underwent comprehensive physiological assessment with right-sided heart catheterization and radionuclide ventriculography at rest and during exercise. Our findings were validated in a second cohort undergoing invasive hemodynamic evaluations (n = 71), as well as in an independent cohort with or without known pulmonary arterial (PA) hypertension (n = 30).

RESULTS—In the discovery cohort, 21 metabolites were associated with 2 or more hemodynamic indicators of RV-PV function (i.e., resting right atrial pressure, mean PA pressure,

REPRINT REQUESTS AND CORRESPONDENCE: Dr. Gregory D. Lewis, Cardiology Division, Massachusetts General Hospital, Bigelow 800, Fruit Street, Boston, Massachusetts 02114. glewis@partners.org. OR Dr. Robert E. Gerszten, Cardiovascular Research Center, Massachusetts General Hospital, CPZ 185, 185 Cambridge Street, Boston, Massachusetts 02114. rgerszten@partners.org OR Gerszten.Robert@mgh.harvard.edu.

All other authors have reported that they have no relationships relevant to the contents of this paper to disclose.

APPENDIX For an expanded Methods section as well as additional tables and figures, please see the online version of this article.

pulmonary vascular resistance [PVR], and PVR and PA pressure-flow response [ΔPQ] during exercise). We identified novel associations of RV-PV dysfunction with circulating indoleamine 2,3-dioxygenase (IDO)–dependent tryptophan metabolites (TMs), tricarboxylic acid intermediates, and purine metabolites and confirmed previously described associations with arginine–nitric oxide metabolic pathway constituents. IDO-TM levels were inversely related to RV ejection fraction and were particularly well correlated with exercise PVR and ΔPQ. Multisite sampling demonstrated transpulmonary release of IDO-TMs. IDO-TMs also identified RV-PV dysfunction in a validation cohort with known risk factors for pulmonary hypertension and in patients with established PA hypertension.

CONCLUSIONS—Metabolic profiling identified reproducible signatures of RV-PV dysfunction, highlighting both new biomarkers and pathways for further functional characterization.

Keywords

exercise; hemodynamics; metabolism; pulmonary circulation

There is an unmet clinical need to develop new circulating biomarkers of pulmonary hypertension (PH). Novel biomarkers of right ventricular (RV)–pulmonary vascular (PV) dysfunction might aid in earlier PH detection and inform selection of patients for PH-specific therapies, while reducing reliance on subjective measures (e.g., functional class) and invasive hemodynamic assessment. The profiling of metabolites, including lipids, sugars, nucleotides, amino acids, and amines, is particularly relevant to the understanding of RV-PV dysfunction. Studies in both experimental models and patients have suggested a maladaptive imbalance between pulmonary vasodilators and vasoconstrictors in RV-PV dysfunction. Several small-molecule mediators of PV tone have been identified, including the nitric oxide (NO) second messenger cyclic guanosine monophosphate, prostaglandins, and other biogenic amines (1–3). PV remodeling and right ventricular (RV) hypertrophy have been associated with a potential switch from fatty acid oxidation to glycolysis (4,5), which provides further motivation to apply a more global metabolite profiling approach to PH. Ultimately, metabolite profiling might highlight measures to redress metabolic derangements in RV-PV dysfunction (6,7).

In this study, we hypothesized that simultaneous invasive hemodynamic measurements during right-sided heart catheterization and blood sampling in dyspneic subjects would permit derivation of metabolic signatures of RV-PV dysfunction. We recruited subjects with dyspnea and a wide range of right-sided heart catheterization hemodynamic profiles, as well as predefined groups of people with and without known World Health Organization Group 1 pulmonary arterial hypertension (PAH), to identify metabolite profiles of RV-PV dysfunction. We performed blood sampling in multiple anatomic sites to localize the source of metabolic signatures. To optimize the precision of our phenotyping of RV-PV dysfunction, we also measured the degree of impairment in exercise capacity (peak oxygen uptake [V_{O_2}]) and performed minute-by-minute hemodynamic measurements across varying RV loading conditions during exercise to probe the capacity of the RV-PV unit to accommodate increased blood flow (8). Furthermore, we used a well-described animal

model to evaluate the expression of key enzymes and metabolites in an emerging pathway associated with PH in our human studies.

METHODS

We enrolled 2 consecutive cohorts of patients who underwent cardiopulmonary exercise testing (CPET) with invasive hemodynamic monitoring at Massachusetts General Hospital to evaluate dyspnea on exertion. Patients provided informed consent to participate in this study. Exclusion criteria consisted of the following: 1) left ventricular (LV) systolic dysfunction (left ventricular ejection fraction [LVEF] <0.45) or severe valvular heart disease; 2) chronic kidney disease (worse than stage 3); 3) parenchymal lung disease with a pulmonary mechanical limitation to exercise as defined by minute ventilation (V_E)/(forced expiratory volume in 1 s [FEV_1] × 35) >0.7 at the ventilatory anaerobic threshold (9); or 4) incomplete pulmonary arterial catheter pressure measurements.

A third cohort was prospectively recruited from patients referred to the Vanderbilt Pulmonary Hypertension Clinic who were diagnosed with right-sided heart catheterization–proven PAH attributable to idiopathic, heri-table, drug- or toxin-associated, or connective tissue disease–associated PAH and who provided consent for having their blood drawn. The control subjects were recruited prospectively from an e-mail distribution to all Vanderbilt employees seeking healthy individuals of similar age, sex, and body mass index (BMI) to enroll as control subjects in their PAH clinic blood sampling study. The human studies were approved by the Partners Healthcare System and Vanderbilt University Institutional Review Boards.

Subjects in the first 2 cohorts were mandated to be fasting for at least 8 h before CPET and blood draws for metabolite measurements. Invasive CPET with first-pass radionuclide ventriculography was performed as described previously (7,10) (Online Appendix, Online Figure 1). In the third PAH versus control validation cohort, peripheral venous plasma samples were obtained in the fasting state at 3 (median interquartile range: 0 to 6) days from the time of right-sided heart catheterization documenting PAH.

Profiles of plasma metabolites were obtained by use of a multiplexed liquid chromatography mass spectrometry (LC-MS) system as described previously (11) (Online Appendix). Additionally, commercially available enzyme-linked immunosorbent assays were used to measure N-terminal pro–B-type natriuretic peptide (NT-proBNP), cystatin C, and interleukin (IL)-6 levels from separate aliquots of the same samples used for LC-MS analysis of metabolites.

ANIMAL MODEL OF PH

Male C57Bl/6 mice (8 to 10 weeks old) were obtained from the Jackson Laboratory (Bar Harbor, Maine). Mice were housed in specially designed cage racks and exposed to chronic hypoxia (FIO_2 0.10) or room air (control) for 3 weeks. All animal studies were approved by the Institutional Animal Care and Use Committee of the Massachusetts General Hospital and conformed to the position of the American Heart Association on animal use. After mice were euthanized, blood was collected via LV puncture, and a thoracotomy was performed

for heart and lung harvesting. RV hypertrophy was calculated as the ratio of the RV wall weight to LV wall plus septum weight (RV/[LV + S] × Fulton ratio).

Blood samples from the mice were centrifuged at 8,000 revolutions/min for 5 min at 4°C. Plasma was immediately stored at −80°C. Lung tissue was snap frozen in liquid nitrogen immediately after harvest and stored at −80°C. For homogenization of the lung, 25 mg of tissue sample was mixed with 250 μl of 50:50 methanol:water solution. The tissue was homogenized for 4 min at 25 Hz in the Tissue Lyser II (Qiagen, Hilden, Germany). Metabolite profiling was performed on plasma and lung homogenate as described previously for the human plasma samples. Indoleamine 2,3-dioxygenase-dependent (IDO) ribonucleic acid (RNA) content was measured by quantitative real-time polymerase chain reaction (Online Appendix).

STATISTICAL ANALYSES

All metabolite values and NT-proBNP levels were log-transformed because of non-normal distribution. Age- and sex-adjusted Pearson correlation coefficients were calculated to determine correlations between metabolites known to cluster within well-defined groups (e.g., arginine-NO metabolites and tryptophan metabolites). Linear regression analyses were performed to examine the relation of each metabolite with hemodynamic measurements that reflect RV-PV function: right atrial pressure (RAP), pulmonary arterial pressure (PAP), and pulmonary vascular resistance (PVR) at rest, and PVR and change in mean PAP relative to change in cardiac output (ΔPQ) during exercise. Relationships between metabolites and pulmonary arterial wedge pressure (PAWP) are included for the sake of comparison of metabolite relationships to left-sided heart filling pressures.

Multimarker scores were created for metabolites that cluster into known metabolic pathways if multiple constituents demonstrated significant associations with hemodynamic indicators of RV-PV function. Scores were derived by calculating the sum of standardized biomarker values (*z*-scores) weighted according to the value of their corresponding β-coefficients, as described previously (11). Multimarker scores fit to the derivation cohort that were significantly associated with RV-PV dysfunction were then evaluated by linear regression in the second validation cohort. Receiver operating coefficient analyses were performed to identify the ability of metabolites to predict RV-PV dysfunction in the validation cohort. The C-statistic was calculated by assessing the proportion of cases (RV-PV dysfunction) for which the biomarker value exceeded that in controls (no RV-PV dysfunction).

To further validate novel circulating metabolites in an independent cohort, we compared levels of IDO tryptophan metabolites (IDO-TMs) in patients with known PAH and control subjects. To have 80% power to detect a 20% difference in 4 IDO-TMs with $p < 0.0125$ (Bonferroni correction $p = 0.05$ for 4 metabolites) between groups, we performed metabolite profiling in 11 patients with PAH and 19 control subjects. Between-group comparisons were performed for the PAH versus control cohort with Student *t* test or Wilcoxon rank sum test, as appropriate. Additional information regarding adjustment for multiple hypothesis testing and regression models is available in the Online Appendix. The STATA version 12.0 software package (StataCorp LP, College Station, Texas) was used for statistical analysis.

RESULTS

CLINICAL CHARACTERISTICS

Study participants undergoing CPET had an average age of 62 years in both cohorts, with a slight female predominance (Table 1). Average resting right-sided heart catheterization measurements were in the high-normal range. No patients demonstrated LV systolic dysfunction, as defined by either an LVEF <0.45 at rest or a fall in LVEF to <0.45 during exercise. Exercise unmasked impaired RV-PV reserve function in both the derivation and validation groups, as evidenced by multipoint changes in ΔPQ and peak exercise PVR (Table 1). In the setting of these hemodynamic profiles, average exercise capacity was reduced in both the derivation and validation cohorts (peak V_{O_2} = 62 ± 13% predicted and 66 ± 14% predicted (12), respectively).

ANALYTES ASSOCIATED WITH RV-PV DYSFUNCTION

We measured 5 hemodynamic indicators of RV-PV dysfunction (resting RAP, PAP, PVR, exercise PVR, and ΔPQ). We integrated the hemodynamic measurements with mass spectrometry–based analyses of metabolites (Figure 1), identifying 21 metabolites that were significantly associated with 2 or more measurements of RV-PV dysfunction in a regression analysis ($p < 0.0095$ for each analyte).

Many metabolites clustered within previously defined pathways. Levels of arginine-NO metabolites (Arg-Ms: arginine, ornithine, citrulline, asymmetric dimethylarginine, and symmetric dimethylarginine) were related to indexes of RV-PV dysfunction (Figure 1, Table 2). The ratio of arginine to ornithine + citrulline, which reflects global arginine bioavailability and has emerged as a potential PH biomarker in select PH populations with sickle cell disease (13) and heart failure (1), was inversely related to PAP, PVR, and ΔPQ (all $p < 0.005$) (Table 2). A cluster of purine degradation products (i.e., purine-Ms: allantoin, xanthosine, inosine, xanthine, uric acid) was also closely related to RV-PV dysfunction. Several of these purine-Ms are associated with oxidative stress, although only urate has been associated with PH (14).

The amino acid tryptophan can be metabolized via 2 enzymatic pathways: tryptophan hydroxylase (TH), which yields serotonin (5-hydroxytryptophan) and the main metabolite of serotonin (5-hydroxyindoleacetic acid), or via IDO, which generates kynurenine, anthranilate, kynurenate, and quinolinate. We identified striking associations between RV-PV dysfunction and IDO-TMs (Figure 1, Table 2) that have not previously been associated with PH. By contrast, tryptophan metabolites downstream from TH were not related to hemodynamic indexes of RV-PV dysfunction (Figure 1). Additionally, plasma levels of tricarboxylic acid (TCA) cycle metabolites (TCA-Ms) were closely associated with hemodynamic indexes of RV-PV dysfunction. Although TCA intermediates generally function intracellularly, we have previously documented that these metabolites are detectable in plasma (15).

We next assessed interpathway and intrapathway correlations. Relationships across annotated pathways are displayed in Online Table 1. Moderate correlations within groups of related metabolites were observed for IDO-TMs, TCA-Ms, purine-Ms, and Arg-Ms, whereas

TH-TMs were not strongly interrelated. Although many of the metabolites highlighted by the LC-MS based platform fell into previously described pathways, other metabolites had less obvious metabolic connections (Figure 1). We identified associations between indexes of RV-PV dysfunction and the catecholamine vanillylmandelic acid, as well as aminoisobutyric acid and cyclic adenosine monophosphate, 2 additional metabolites potentially related to sympathetic nervous system activation (16,17). Plasma levels of the homocysteine metabolite cystathionine, as well as glyceraldehyde and glucoronate, were also related to indexes of RV-PV dysfunction.

MULTIMARKER SCORES

To assess how clusters of metabolites from a given metabolic pathway relate to hemodynamic measurements, composite scores were generated by summing *z*-scores of individual metabolites weighted by β-coefficients within clusters (18) (Table 2). Composite scores from each group, adjusted for age and sex, were closely related to PAP and PVR at rest (Table 2). By contrast, none of the metabolite scores were significantly associated with systemic MAP (data not shown). Although purine-Ms and Arg-Ms demonstrated similar β-coefficients for PAP and PAWP, IDO-TMs and TCA-Ms demonstrated β-coefficients <0.3 with PAWP and ≥0.4 for PAP, which suggests relative specificity for pre-capillary PAP as opposed to PAP driven by left-sided filling pressure. Moreover, IDO scores remained associated with PAP, PVR, and ΔPQ ($p < 0.05$) after adjustment for each of the other pathway scores. Individuals in the top quartile of the IDO-TM score had a 2.9-fold greater ΔPQ (Figure 2) and a 2.2-fold greater PVR at rest and with exercise (p for trend < 0.001 for all). IDO-TMs remained significantly related to indexes of RV-PV dysfunction after further adjustment for NT-proBNP, a marker of myocardial wall stress and PH (19); cystatin C, indicative of renal function; and IL-6, an inflammatory cytokine previously associated with PH (Table 3). After stepwise adjustment for the combination of age, sex, NT-proBNP, cystatin C, and IL-6, IDO-TM scores remained significantly associated with RAP, mPAP, PVR, exercise PVR, and ΔPQ ($p \leq 0.01$ for all) (Table 3). Of the 4 IDO-TMs, only kynurenate was significantly associated with serum creatinine ($\beta = 0.41$; $p = 0.003$). Furthermore, IDO-TM scores were not significantly associated with BMI, diabetes, hypertension, smoking status, or exposure to beta-blockers, angiotensin-converting enzyme inhibitors/angiotensin receptor blockers, calcium channel blockers, diuretic agents, statins, aspirin, or warfarin ($p > 0.1$ for all) (Online Table 2).

The novel finding in humans that IDO-dependent metabolites are closely related to indexes of RV-PV dysfunction led us to further examine their relationship with other indicators of RV-PV dysfunction beyond hemodynamic variables. IDO-TM composite scores were inversely associated with right ventricular ejection fraction (RVEF) ($\beta = 0.38$, $p = 0.007$), and the association with RVEF remained significant after adjustment for age, sex, and NT-proBNP levels ($p = 0.015$). Furthermore, because exercise intolerance is a cardinal manifestation of RV-PV dysfunction, and reduced peak V_{O_2} is associated with poor prognosis in various forms of PH (20–22), we examined whether IDO-TMs also predicted impaired exercise capacity. We found that higher levels of IDO-TMs were associated with reduced percent-predicted peak V_{O_2}, even after adjusting for NT-proBNP ($\beta = 0.36$; $p =$

0.009). IDO-TMs thus provide markers of RV-PV dysfunction that signal both hemodynamic impairment and reduced functional capacity.

LOCALIZATION OF METABOLIC CHANGES IN HUMAN STUDIES

To examine whether there was net uptake or release of IDO-TMs across the pulmonary circulation, we examined relative concentrations of the 4 IDO-TMs in radial arterial and proximal pulmonary arterial samples. In subjects with normal resting PVR, there were no significant differences in pulmonary and radial arterial levels of IDO-TMs (Figure 3); however, subjects with elevated PVR (>2 Wood units) demonstrated significantly higher radial arterial levels of kynurenine, anthranilate, and quinolinate than pulmonary arterial levels ($p < 0.05$ for all), which indicates release of these metabolites into the pulmonary circulation. The observed gradient in IDO-TMs across the pulmonary circulation in individuals with elevated PVR suggests a pulmonary origin of the observed increases in circulating IDO-TMs in patients with PV dysfunction.

LOCALIZATION OF METABOLIC CHANGES IN AN ANIMAL MODEL

To add information regarding tissue specificity, IDO and IDO-TMs were examined in lung tissue from an experimental animal model of hypoxia-induced PH (Figure 4). RV hypertrophy was confirmed by an elevated Fulton ratio of 0.35 ± 0.02 in the hypoxia group versus 0.22 ± 0.02 in controls ($p < 0.001$). Lung messenger RNA expression of IDO was 2.5-fold higher in mice with PH than in controls ($p < 0.001$) (Figure 4A); the IDO substrate-product ratio was elevated in lung tissue ($p < 0.001$) (Figure 4B); plasma levels of IDO-TMs were elevated in experimental PH (mean *z*-score: 0.42 vs. −0.50, $p = 0.004$) (Figure 4C), and their degree of elevation was closely correlated to Fulton ratios ($r = 0.48$ to 0.72; all $p < 0.05$).

ADDITIONAL VALIDATION STUDIES

We assessed the performance of our metabolite biomarkers in a second set of CPET subjects who served as a validation cohort. Multimarker combinations of metabolites associated with RV-PV dysfunction, identical to those identified in the derivation cohort (Table 2), demonstrated significant associations with indexes of RV-PV dysfunction in the validation cohort, with the majority of β-coefficients >0.25 and $p < 0.05$ (Table 4). We subsequently stratified the validation group according to whether or not abnormal pulmonary vascular function was present (+PH; $n = 35$), as evidenced by mPAP ≥21 mm Hg with PVR >2.0 Wood Units and ΔPQ >3.0 mm Hg/l/min (8–11,23,24), or absent (−PH; $n = 36$). Receiver operating characteristic curves generated for each IDO-TM in the validation cohort demonstrated C-statistics that ranged from 0.66 to 0.74 (Figure 5A). IDO-TMs retained their significance in logistic regression models that included variables known to be associated with PH (age, sex, BMI, RVEF, and PAWP), with C-statistic increments ranging from 0.02 to 0.09 (Table 5).

To further assess the performance of IDO-TMs as potential markers of RV-PV dysfunction, we also examined IDO-TM levels in an independent cohort of patients with known World Health Organization Group 1 PAH and control subjects of similar age, sex, and BMI (Table 6). The 3 IDO-TMs with transpulmonary release in the high-PVR group (anthranilate,

quinolinate, and kynurenine) demonstrated significantly higher levels in PAH, with C-statistics of 0.79 to 0.86 (Figure 5B); kynurenate did not differ between groups.

DISCUSSION

Metabolite profiling permits comprehensive, relatively unbiased investigation of metabolic pathways that potentially underlie complex phenotypes such as RV-PV dysfunction. Using a mass spectrometry–based metabolite profiling platform, we identified a panel of metabolites for which the plasma concentrations were closely associated with RV-PV dysfunction. Our platform highlighted small molecules previously associated with RV-PV dysfunction, including arginine-NO pathway intermediates, catecholamines, and indicators of oxidative stress. Furthermore, we identified circulating metabolites (TCA cycle intermediates and IDO-TMs) not previously associated with RV-PV dysfunction in humans (Central Illustration), which represent novel potential biomarkers of PH. IDO-TMs are particularly attractive potential markers of RV-PV dysfunction because of their transpulmonary release in patients with high PVR, their relationship with RVEF and steep PQ, and their elevation in human and experimental PAH. Taken together, our data indicated that metabolite profiling may provide biomarkers of PV disease and a window into the metabolic pathways altered in RV-PV dysfunction.

A growing number of studies have evaluated potential circulating biomarkers of PV disease (25,26); however, studies to date have been largely limited to 1 or a few analytes that are compared to single resting noninvasive estimates or measurements of right-sided heart hemodynamics (1,14,27). A strength of our investigation was the application of a well-established targeted LC-MS metabolite profiling platform to measure more than 100 metabolites in carefully phenotyped derivation and validation cohorts. Our analysis benefited from blood sampling performed in parallel with “gold standard” invasive hemodynamic measurements at rest. We also characterized multipoint pressure-flow (PQ) relationships during exercise to further refine patient phenotypes related to RV-PV function (Online Figure 1). Our group and others have recently reported that ΔPQ responses to exercise predict functional capacity and outcomes (8,23,28,29). By linking metabolic signatures to PQ responses indicative of PV reserve capacity, we may gain insight into early markers of RV-PV dysfunction. Ultimately, biomarkers of RV-PV dysfunction will provide the greatest utility if they can differentiate early forms of PH before overt disease ensues.

We found that the ratio of arginine to ornithine + citrulline (Arg/[Orn+Cit]), which reflects global arginine bioavailability, was strongly inversely related to PAP, PVR during rest and exercise, and PQ (Figure 1, Table 2). These findings extend previous work demonstrating that Arg/(Orn+Cit) ratio is a marker of PH severity in select PH-populations with sickle cell disease (13) and LV systolic dysfunction (1). Our study documented a novel association of these metabolites with pulmonary hemodynamic measurements in an unselected population with exertional dyspnea. The particularly strong relationship between Arg/(Orn+Cit) levels and ΔPQ suggested that this ratio may signal impaired NO-mediated vasodilation.

In contrast to arginine pathway metabolites, the association of IDO-TMs with PH in humans has not been established. The consistent, strong correlations between the 4 IDO-TMs and

indexes of RV-PV dysfunction, coupled with their transpulmonary release and association with RVEF, suggest that these markers have specificity for the pulmonary circulation. IDO has a known immunomodulatory role upon induction by proinflammatory stimuli, including interferon-γ, and is expressed in fibroblasts, macrophages, and vascular endothelium (30). The IDO-product kynurenine was identified as a potential endothelium-derived vasodilator in a murine sepsis model (31). In vitro studies by the same group demonstrated that kynurenine triggered dilation of previously constricted porcine arteries. Recently, IDO expression was localized to pulmonary endothelium in mouse lung, and mice lacking the IDO gene demonstrated exaggerated hypoxic pulmonary vasoconstriction (32). Enhanced endothelial IDO ameliorated PH in preclinical models, modulating PH-derived pulmonary artery smooth muscle cells toward a proapoptotic and less proliferative/synthetic state. However, to the best of our knowledge, there have been no studies linking this pathway to human disease.

IDO-TMs may be released as vasodilators in response to PH just as natriuretic peptides are secreted in the setting of myocardial wall stretch. As a heme-containing enzyme, IDO may be inhibited by NO (33), and it is plausible that production of IDO-TMs represents a compensatory pathway activated in states of NO deficiency, such as RV-PV dysfunction. Our finding that IDO-TMs were inversely correlated with plasma markers of Arg-NO bioavailability (Online Table 1) supported this hypothesis, although further investigation of the relationship between NO-deficient states and heightened IDO activity is needed. In contrast to our findings related to IDO-TMs and RV-PV dysfunction, we observed no significant relationship between levels of TH-TMs and RV-PV dysfunction. Serotonin (5-hydroxytryptamine) and the serotonin metabolite 5-hydroxyindoleacetic acid are tryptophan metabolites formed in pulmonary artery endothelial cells by TH (Figure 4A). These metabolites may contribute to pulmonary vasoconstriction and proliferation of pulmonary artery smooth muscle cells, but their storage in platelets and low abundance in plasma make them challenging and often unreliable to measure as PH biomarkers (2,34).

Plasma levels of TCA cycle intermediates, like IDO-TMs, were closely associated with hemodynamic indexes of RV-PV function in our study. Although the TCA cycle is operative within intracellular compartments, we have previously demonstrated that TCA cycle intermediates are detectable in plasma (35,36). Until recently, however, a potential role of TCA cycle intermediates in signaling biologic activity in a hormone-like role was unrecognized. A seminal study by He et al. (18) demonstrated that the span 1 TCA cycle intermediate succinate was sufficient to augment blood pressure in mice by activating a novel G protein–coupled receptor in the kidney. This group hypothesized that release of succinate in the setting of tissue ischemia may serve as a compensatory, protective mechanism to maintain systemic blood pressure. Recently, Zhao et al. (36) utilized pathological specimens from explanted or resected lungs and found elevated TCA cycle intermediates in lungs with severe PAH. Our study extends these findings by showing directionally concordant elevations in TCA cycle intermediates measured in plasma in patients with less advanced PV disease. Ours is the first study to relate circulating levels of succinate and other TCA cycle intermediates to PH, which raises the possibility that succinate or potentially other TCA-related metabolites could modulate vascular tone in humans.

There is mounting evidence of abnormal mitochondrial function, both within and outside the pulmonary circulation in PH. Beyond a well-recognized glycolytic shift that occurs in PH (37), down-regulation of the mitochondrial deacetylase sirtuin 3 has also been implicated in mitochondrial dysfunction in PH (38). The extent to which circulating TCA cycle or glycolytic intermediates accurately reflect mitochondrial dysfunction in PH will be an important area of future investigation.

We also found that metabolites that may relate to sympathetic nervous system activation tracked with RV-PV dysfunction (i.e., vanillylmandelic acid, cyclic adenosine monophosphate, and aminoisobutyric acid). These findings are consistent with previous studies relating heightened catecholamine levels to pulmonary vasoconstriction (17).

STUDY LIMITATIONS

We used a liquid chromatography tandem mass spectrometry platform that provides key "sentinels" across known metabolic pathways but does not fully cover the entire plasma metabolome. Our study design focused on subjects with dyspnea on exertion in the main derivation and validation cohorts, as opposed to a narrowly defined patient population with PH, which resulted in heterogeneity in pathogenesis and degree of PH in our cohort. However, because PH purports a poor prognosis regardless of pathogenesis, biomarkers will be most useful in their application to patients with suspected, as opposed to confirmed, pulmonary vascular disease. Thus, our focus on dyspneic patients is advantageous in this regard. Identification of patients with clear evidence of pulmonary vascular disease in our second validation cohort demonstrated that these biomarkers performed particularly well in separating patients with clear evidence of PAH from those without RV-PV dysfunction (Figure 5). Evaluation of metabolite profiles during exercise warrants future study as a potential way to further improve the specificity of metabolite signatures for impaired RV-PV reserve capacity.

Accounting for potential confounders is of critical importance in a biomarker discovery study. Renal dysfunction in particular is associated with increases in several circulating metabolites, including tryptophan metabolites that are known to be increased in the setting of uremia (39). We excluded patients with advanced kidney disease, and average creatinine levels were normal in both our derivation and validation cohorts (1.1 mg/dl in each). Furthermore, we adjusted for cystatin C concentrations and found that IDO-TM, but not other TMs such as indoxysulfate, remained strongly predictive of pulmonary hemodynamic measurements. Simultaneous peripheral venous and central venous sampling was not available to permit comparison of metabolite levels from the 2 sampling sites. The small sample size of the validation cohort limited our power to identify additional metabolites that may have differed between PAH and control subjects. Finally, in our animal model studies, we acknowledge that the cellular source of metabolites within the lung was not localized, and we did not include invasive hemodynamic measurements to document the degree of PH elicited by hypoxia. However, Fulton ratios were similar to those in other studies in which a >2-fold increment in PAP was obtained (33).

CONCLUSIONS

The present study demonstrated the potential value of integrating metabolomic and clinical data in human cohorts who underwent detailed phenotyping while identifying small-molecule reporters of RV-PV function. This study begins to address an unmet clinical need to develop noninvasive markers of RV-PV function and reserve capacity. Novel markers of RV-PV functional reserve may aid in earlier detection of RV-PV dysfunction and help to quantify the burden of RV-PV dysfunction in patients with cardiopulmonary diseases.

Supplementary Material

Refer to Web version on PubMed Central for supplementary material.

Acknowledgments

This work was supported by National Institutes of Health (NIH) grants 1R01 HL098280 and R01 DK081572 (Bethesda, Maryland) and the Leducq Foundation. The project was also supported by Clinical and Translational Science Award No. UL1TR000445 (Dr. Hemnes and Dr. Pugh) from the National Center for Advancing Translational Sciences (Bethesda, Maryland). Its contents are solely the responsibility of the authors and do not necessarily represent official views of the National Center for Advancing Translational Sciences or the NIH. Dr. Lewis was supported by NIH grants K23HL091106, NIH R01 HL131029, and NIH R01 HL119154 (Bethesda, Maryland), American Heart Association (AHA) grant 15GPSGC24800006 (Dallas, Texas), and the Hassenfeld Clinical Scholar Award (Boston, Massachusetts). Dr. Pugh has served as an advisory board member for Gilead. Dr. Gerszten was supported by an AHA Established Investigator Award (Dallas, Texas).

ABBREVIATIONS AND ACRONYMS

BMI	body mass index
CPET	cardiopulmonary exercise test
ΔPQ	change in mean pulmonary arterial pressure relative to change in cardiac output
IDO	indoleamine 2,3-dioxygenase
IDO-TM	indoleamine 2,3-dioxygenase–dependent tryptophan metabolite
IL	interleukin
LC-MS	liquid chromatography mass spectrometry
LV	left ventricular
LVEF	left ventricular ejection fraction
NO	nitric oxide
NT-proBNP	N-terminal pro–B-type natriuretic peptide
PAH	pulmonary arterial hypertension
PAP	pulmonary arterial pressure
PAWP	pulmonary arterial wedge pressure

PH	pulmonary hypertension
PV	pulmonary vascular
PVR	pulmonary vascular resistance
RAP	right atrial pressure
RNA	ribonucleic acid
RV	right ventricular
RVEF	right ventricular ejection fraction
RV-PV	right ventricular-pulmonary vascular
TCA	tricarboxylic acid
TH	tryptophan hydroxylase
TM	tryptophan metabolite

REFERENCES

1. Shao Z, Wang Z, Shrestha K, et al. Pulmonary hypertension associated with advanced systolic heart failure: dysregulated arginine metabolism and importance of compensatory dimethylarginine dimethylaminohydrolase-1. J Am Coll Cardiol. 2012; 59:1150–8. [PubMed: 22440215]
2. Herve P, Launay JM, Scrobohaci ML, et al. Increased plasma serotonin in primary pulmonary hypertension. Am J Med. 1995; 99:249–54. [PubMed: 7653484]
3. Galie N, Manes A, Branzi A. Prostanoids for pulmonary arterial hypertension. Am J Respir Med. 2003; 2:123–37. [PubMed: 14720012]
4. Xu W, Koeck T, Lara AR, et al. Alterations of cellular bioenergetics in pulmonary artery endothelial cells. Proc Natl Acad Sci U S A. 2007; 104:1342–7. [PubMed: 17227868]
5. Takeyama D, Kagaya Y, Yamane Y, et al. Effects of chronic right ventricular pressure overload on myocardial glucose and free fatty acid metabolism in the conscious rat. Cardiovasc Res. 1995; 29:763–7. [PubMed: 7656279]
6. Stasch JP, Pacher P, Evgenov OV. Soluble guanylate cyclase as an emerging therapeutic target in cardiopulmonary disease. Circulation. 2011; 123:2263–73. [PubMed: 21606405]
7. Lewis GD, Shah R, Shahzad K, et al. Sildenafil improves exercise capacity and quality of life in patients with systolic heart failure and secondary pulmonary hypertension. Circulation. 2007; 116:1555–62. [PubMed: 17785618]
8. Lewis GD, Bossone E, Naeije R, et al. Pulmonary vascular hemodynamic response to exercise in cardiopulmonary diseases. Circulation. 2013; 128:1470–9. [PubMed: 24060943]
9. Hansen JE, Sue DY, Wasserman K. Predicted values for clinical exercise testing. Am Rev Respir Dis. 1984; 129(2 Pt 2):S49–55. [PubMed: 6421218]
10. Lewis GD, Lachmann J, Camuso J, et al. Sildenafil improves exercise hemodynamics and oxygen uptake in patients with systolic heart failure. Circulation. 2007; 115:59–66. [PubMed: 17179022]
11. Wang TJ, Larson MG, Vasan RS, et al. Metabolite profiles and the risk of developing diabetes. Nat Med. 2011; 17:448–53. [PubMed: 21423183]
12. Jones NL, Makrides L, Hitchcock C, Chypchar T, McCartney N. Normal standards for an incremental progressive cycle ergometer test. Am Rev Respir Dis. 1985; 131:700–8. [PubMed: 3923878]
13. Morris CR, Kato GJ, Poljakovic M, et al. Dysregulated arginine metabolism, hemolysis-associated pulmonary hypertension, and mortality in sickle cell disease. JAMA. 2005; 294:81–90. [PubMed: 15998894]

14. Nagaya N, Uematsu M, Satoh T, et al. Serum uric acid levels correlate with the severity and the mortality of primary pulmonary hypertension. Am J Respir Crit Care Med. 1999; 160:487–92. [PubMed: 10430718]
15. Lewis GD, Farrell L, Wood MJ, et al. Metabolic signatures of exercise in human plasma. Sci Transl Med. 2010; 2:33ra37.
16. Guazzi MD, De Cesare N, Fiorentini C, et al. Pulmonary vascular supersensitivity to catecholamines in systemic high blood pressure. J Am Coll Cardiol. 1986; 8:1137–44. [PubMed: 3760387]
17. Guazzi MD, Alimento M, Fiorentini C, Pepi M, Polese A. Hypersensitivity of lung vessels to catecholamines in systemic hypertension. Br Med J (Clin Res Ed). 1986; 293:291–4.
18. He W, Miao FJ, Lin DC, et al. Citric acid cycle intermediates as ligands for orphan G-protein-coupled receptors. Nature. 2004; 429:188–93. [PubMed: 15141213]
19. Galiè N, Hoeper MM, Humbert M, et al. Guidelines for the diagnosis and treatment of pulmonary hypertension: the Task Force for the Diagnosis and Treatment of Pulmonary Hypertension of the European Society of Cardiology (ESC) and the European Respiratory Society (ERS), endorsed by the International Society of Heart and Lung Transplantation (ISHLT) [published correction appears in Eur Heart J 2011;32:926]. Eur Heart J. 2009; 30:2493–537. [PubMed: 19713419]
20. Guazzi M, Boracchi P, Arena R, et al. Development of a cardiopulmonary exercise prognostic score for optimizing risk stratification in heart failure: the (P)e(R)i(O)dic (B)reathing during (E) xercise (PROBE) study. J Card Fail. 2010; 16:799–805. [PubMed: 20932461]
21. Wensel R, Opitz CF, Anker SD, et al. Assessment of survival in patients with primary pulmonary hypertension: importance of cardiopulmonary exercise testing. Circulation. 2002; 106:319–24. [PubMed: 12119247]
22. Inuzuka R, Diller GP, Borgia F, et al. Comprehensive use of cardiopulmonary exercise testing identifies adults with congenital heart disease at increased mortality risk in the medium term. Circulation. 2012; 125:250–9. [PubMed: 22147905]
23. Saggar R, Lewis GD, Systrom DM, Champion HC, Naeije R, Saggar R. Pulmonary vascular responses to exercise: a haemodynamic observation. Eur Respir J. 2012; 39:231–4. [PubMed: 22298608]
24. Kovacs G, Berghold A, Scheidl S, Olschewski H. Pulmonary arterial pressure during rest and exercise in healthy subjects: a systematic review. Eur Respir J. 2009; 34:888–94. [PubMed: 19324955]
25. Desai AA, Zhou T, Ahmad H, et al. A novel molecular signature for elevated tricuspid regurgitation velocity in sickle cell disease. Am J Respir Crit Care Med. 2012; 186:359–68. [PubMed: 22679008]
26. Abdul-Salam VB, Paul GA, Ali JO, et al. Identification of plasma protein biomarkers associated with idiopathic pulmonary arterial hypertension. Proteomics. 2006; 6:2286–94. [PubMed: 16493708]
27. Cracowski JL, Leuchte HH. The potential of biomarkers in pulmonary arterial hypertension. Am J Cardiol. 2012; 110(Suppl):32S–8S. [PubMed: 22921030]
28. Lewis GD, Murphy RM, Shah RV, et al. Pulmonary vascular response patterns during exercise in left ventricular systolic dysfunction predict exercise capacity and outcomes. Circ Heart Fail. 2011; 4:276–85. [PubMed: 21292991]
29. Lalande S, Yerly P, Faoro V, Naeije R. Pulmonary vascular distensibility predicts aerobic capacity in healthy individuals. J Physiol. 2012; 590:4279–88. [PubMed: 22733662]
30. Grant R, Kapoor V. Inhibition of indoleamine 2, 3-dioxygenase activity in IFN-gamma stimulated astroglioma cells decreases intracellular NAD levels. Biochem Pharmacol. 2003; 66:1033–6. [PubMed: 12963490]
31. Wang Y, Liu H, McKenzie G, et al. Kynurenine is an endothelium-derived relaxing factor produced during inflammation. Nat Med. 2010; 16:279–85. [PubMed: 20190767]
32. Xiao Y, Christou H, Liu L, et al. Endothelial indoleamine 2,3-dioxygenase protects against development of pulmonary hypertension. Am J Respir Crit Care Med. 2013; 188:482–91. [PubMed: 23822766]

33. Thomas SR, Mohr D, Stocker R. Nitric oxide inhibits indoleamine 2,3-dioxygenase activity in interferon-gamma primed mononuclear phagocytes. J Biol Chem. 1994; 269:14457–64. [PubMed: 7514170]

34. Lederer DJ, Horn EM, Rosenzweig EB, et al. Plasma serotonin levels are normal in pulmonary arterial hypertension. Pulm Pharmacol Ther. 2008; 21:112–4. [PubMed: 17374499]

35. Lewis GD, Wei R, Liu E, et al. Metabolite profiling of blood from individuals undergoing planned myocardial infarction reveals early markers of myocardial injury. J Clin Invest. 2008; 118:3503–12. [PubMed: 18769631]

36. Zhao Y, Peng J, Lu C, et al. Metabolomic heterogeneity of pulmonary arterial hypertension. PLoS One. 2014; 9:e88727. [PubMed: 24533144]

37. Sutendra G, Michelakis ED. The metabolic basis of pulmonary arterial hypertension. Cell Metab. 2014; 19:558–73. [PubMed: 24508506]

38. Paulin R, Dromparis P, Sutendra G, et al. Sirtuin 3 deficiency is associated with inhibited mitochondrial function and pulmonary arterial hypertension in rodents and humans. Cell Metab. 2014; 20:827–39. [PubMed: 25284742]

39. Koenig P, Nagl C, Neurauter G, Schennach H, Brandacher G, Fuchs D. Enhanced degradation of tryptophan in patients on hemodialysis. Clin Nephrol. 2010; 74:465–70. [PubMed: 21084050]

PERSPECTIVES

COMPETENCY IN MEDICAL KNOWLEDGE

In patients with exertional dyspnea, plasma levels of tryptophan breakdown products, tricarboxylic acid cycle intermediaries and purine metabolites correlate with the severity of pulmonary hypertension and right ventricular dysfunction.

TRANSLATIONAL OUTLOOK

Additional research is needed to characterize the pathophysiological pathways by which these and othermetabolites contribute to pulmonary hypertension and dyspnea of hemodynamic origin. Circulating biochemical signatures may ultimately be useful for earlier patient diagnosis or to identify those who might benefit from an intervention.

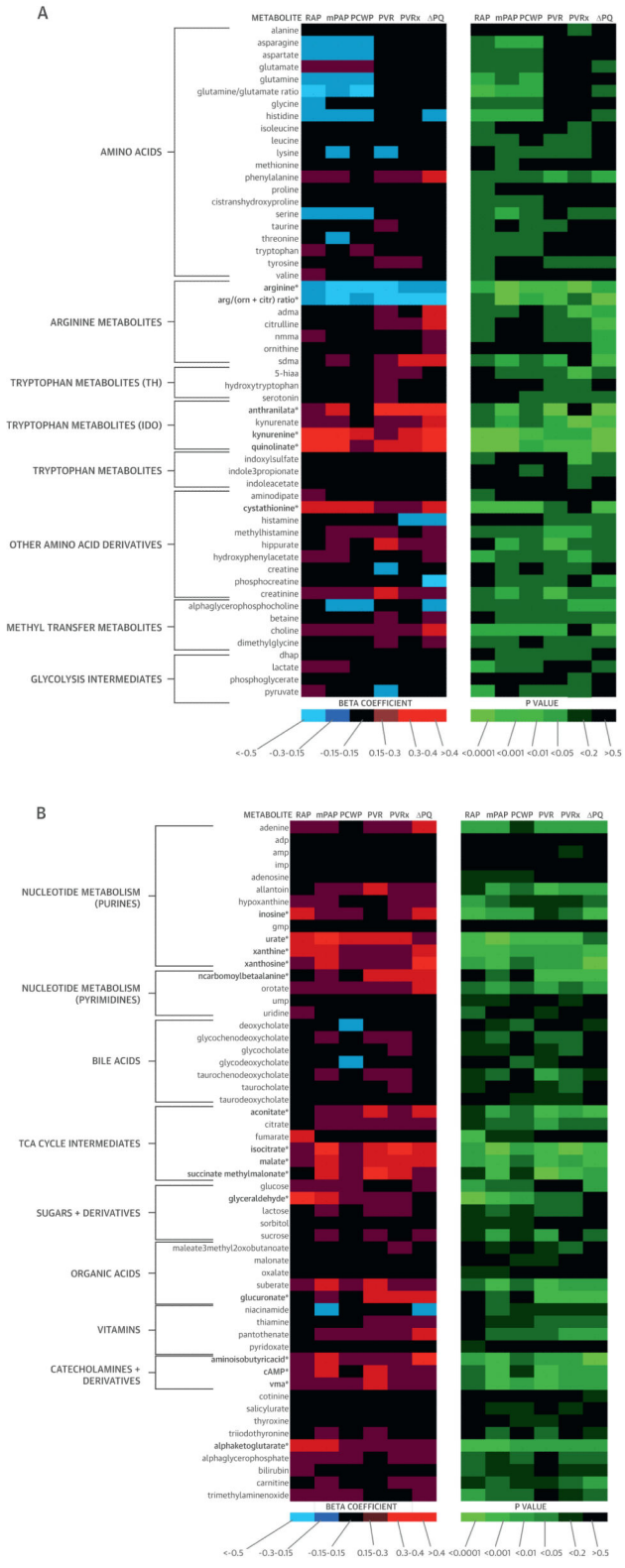

FIGURE 1. Metabolic Heat Map

β-Coefficients and p values generated from regression analyses depict the relationship of each metabolite (log transformed) with hemodynamic measurements. *$p < 0.0095$ for associations with 2 or more measurements of RV-PV dysfunction (see Methods). 5-hiaa = 5-hydroxy-indoleacetic acid; ADMA = asymmetric dimethylarginine; adp = adenosine diphosphate; amp = adenosine monophosphate; arg/(orn + citr) = ratio of arginine to sum of ornithine + citrulline; cAMP = cyclic adenosine monophosphate; ΔPQ = change in pressure relative to change in cardiac output during exercise; dhap = dihydroxyacetone phosphate; gmp = guanosine monophosphate; IDO = indoleamine 2,3-dioxygenase; imp = inosine monophosphate; mPAP = mean pulmonary arterial pressure; PAWP = pulmonary arterial wedge pressure; PCWP = pulmonary capillary wedge pressure; PVR = pulmonary vascular resistance; PVRx = pulmonary vascular resistance during exercise; RAP = right atrial pressure; SDMA = symmetric dimethylarginine; TCA = tricarboxylic acid; TH = tryptophan hydroxylase; ump = uridine monophosphate; vma = vanillylmandelic acid.

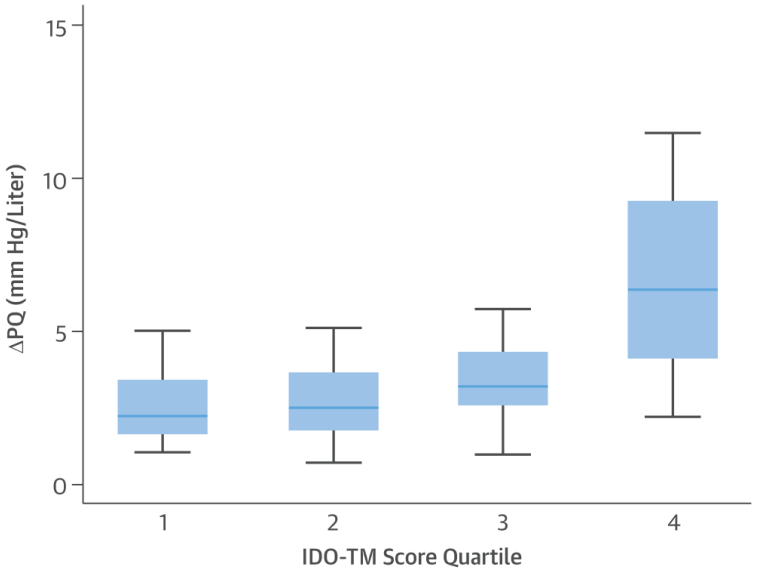

FIGURE 2. Metabolite-ΔPQ Relationship

The highest quartile of indoleamine 2,3-dioxygenase (IDO) tryptophan metabolite (TM) score exhibited a much greater ΔPQ during exercise than the lower quartiles. ΔPQ data = median ± interquartile range of change in mean pulmonary arterial pressure relative to change in cardiac output.

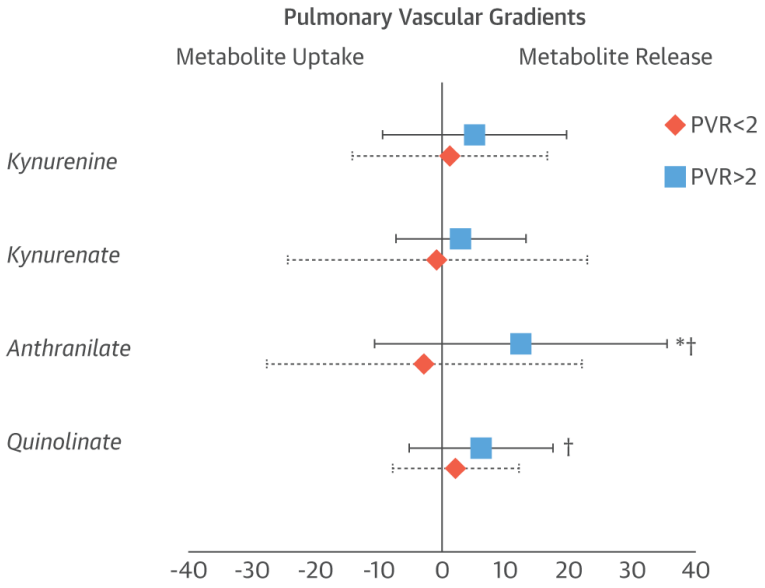

FIGURE 3. Transpulmonary Metabolite Release

For gradients of indoleamine 2,3-dioxygenase tryptophan metabolites across the pulmonary circulation, the average ± SD percent difference in metabolite levels in the radial arterial samples, compared with the pulmonary arterial samples, is indicated for subjects with pulmonary vascular resistance (PVR) ≤2 Wood units (**diamonds**) and >2 Wood units (**squares**). *$p < 0.05$ for PVR ≤2 Wood units versus PVR >2 Wood units; †$p < 0.05$ for PVR >2 Wood units versus no difference.

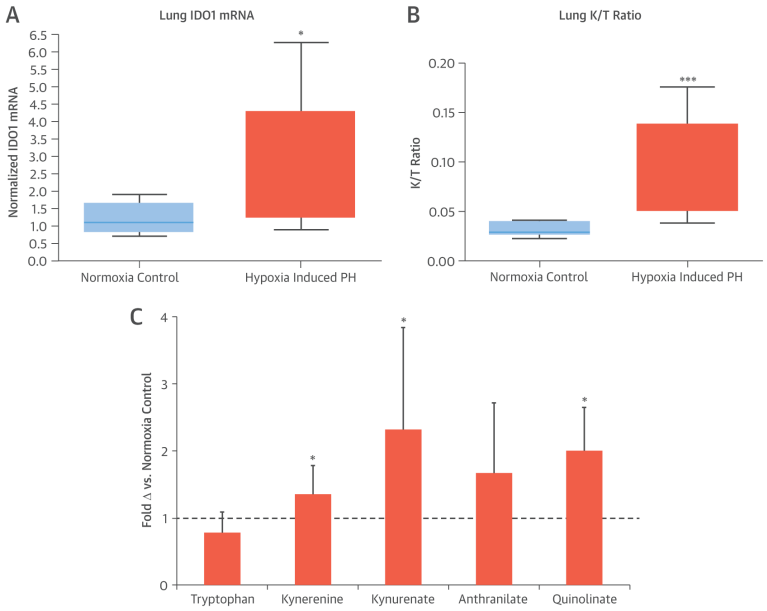

FIGURE 4. Animal Model Studies

(A) Indoleamine 2,3-dioxygenase (IDO1) messenger ribonucleic acid (mRNA) was up-regulated in the lungs of mice with hypoxia-induced pulmonary hypertension (PH) (n = 10) compared with control mice (n = 10). *p = 0.01. **(B)** IDO activity, determined by the ratio of IDO substrate and product (kynurenine/tryptophan [K/T]), was higher in lungs of mice with hypoxia-induced PH (n = 12) than in control mice (n = 10). ***p = 0.002. **(C)** A consistent pattern of elevation in metabolites downstream of IDO was seen in the plasma of mice with hypoxia-induced PH (n = 12) versus control mice (n = 10). *p < 0.05.

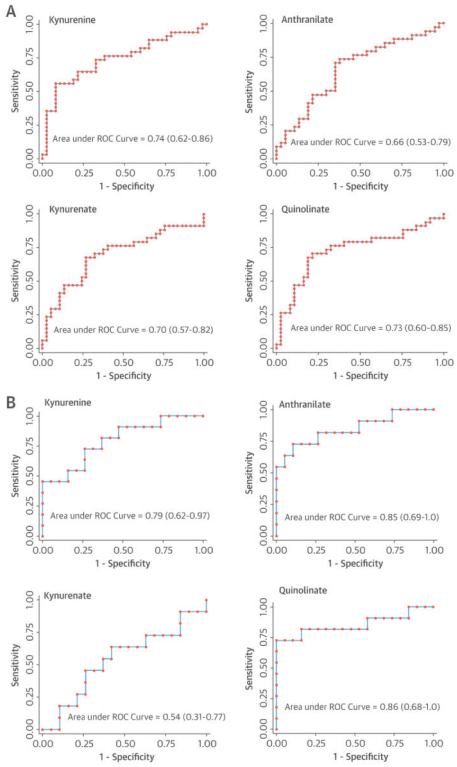

FIGURE 5. ROC Analysis

Receiver-operating characteristic (ROC) curves and area under the curve (with 95% confidence interval) values illustrate the ability of indoleamine 2,3-dioxygenase tryptophan metabolite levels to distinguish **(A)** individuals with and without right ventricular–pulmonary vascular dysfunction in the validation dyspnea cohort stratified by the presence or absence of pulmonary arterial hypertension and **(B)** individuals with known pulmonary arterial hypertension from control subjects in an independent validation cohort.

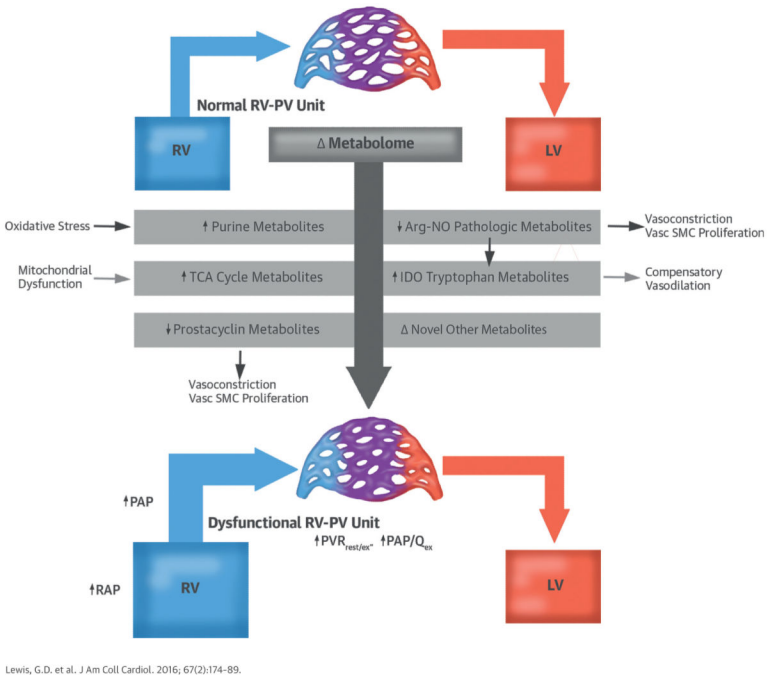

CENTRAL ILLUSTRATION. Metabolic Signatures of Pulmonary Hypertension

Metabolic profiling identified novel associations of right ventricular–pulmonary vascular (RV-PV) dysfunction involving potential new biomarkers and pathways for future research. Arg-NO = arginine nitric oxide; IDO = indoleamine 2-dioxygenase; LV = left ventricle; PAP = pulmonary arterial pressure; PAP/Q_{ex} = pulmonary arterial pressure flow relationship during exercise; PVR = pulmonary vascular resistance; $PVR_{rest/ex}$ = pulmonary vascular resistance during rest and exercise; RAP = right atrial pressure; RV = right ventricle; RV-PV = right ventricular-pulmonary vascular; TCA = tricarboxylic acid; Vasc SMC = vascular smooth muscle cell.

TABLE 1

Clinical Characteristics

	Derivation Cohort (n = 71)	Validation Cohort (n = 71)
Age, yrs	62 ± 13	60 ± 14
Female	62	53
Ethnicity (C, AA, H)	96, 0, 4	96, 1, 3
BMI, kg/m^2	29.2 ± 5.9	28 ± 4.2
Creatinine, g/dl	1.1 ± 0.3	1.1 ± 0.4
Hypertension	58	58
Diabetes mellitus	24	24
Dyslipidemia	49	45
Active smoking	3	10
Active cancer	0	0
Medications		
Beta-blocker	37	31
ACEI/ARB	34	30
CCB	20	12
Diuretic agent	40	31
Statin	42	45
Insulin	10	10
NT-proBNP, pg/ml	820 ± 1,266	662 ± 1,170
RVEF		
At rest	0.50 ± 0.08	0.48 ± 0.07
Exercise	0.50 ± 0.09	0.48 ± 0.07
LVEF		
At rest	0.64 ± 0.09	0.62 ± 0.07
Exercise	0.65 ± 0.08	0.64 ± 0.07
Heart rate, beats/min		
At rest	76 ± 14	77 ± 5
Exercise	128 ± 24	132 ± 29
Systolic BP, mm Hg		
At rest	136 ± 19	142 ± 22
Exercise	182 ± 32	180 ± 38
Diastolic BP, mm Hg		
At rest	79 ± 12	75 ± 13
Exercise	88 ± 15	85 ± 15
Workload, W	90 ± 47	103 ± 49
Peak VO_2, ml/kg/min	15.4 ± 5.8	17.3 ± 6.0
RAP, mm Hg		
At rest	7 ± 3	5 ± 3
Exercise	11 ± 5	11 ± 4
mPAP, mm Hg		

	Derivation Cohort (n = 71)	Validation Cohort (n = 71)
At rest	21 ± 9	23 ± 8
Exercise	38 ± 11	41 ± 13
PAWP, mm Hg		
At rest	13 ± 5	11 ± 5
Exercise	21 ± 6	19 ± 6
Cardiac output, l/min		
At rest	5.5 ± 1.7	5.2 ± 1.5
Exercise	11.6 ± 3.5	11.2 ± 3.6
PVR, WU		
At rest	2.1 ± 1.3	3.1 ± 2.5
Exercise	1.7 ± 1.2	2.2 ± 1.4
ΔPQ, mm Hg/l/min	3.8 ± 2.6	4.5 ± 4.0
PH at rest	20 (28)	27 (38)
ΔPQ >3 mm Hg/l/min	35 (49)	42 (59)
Exercise PVR >1.5 WU	29 (41)	39 (55)

Values are mean ± SD, %, or n (%).

AA = African American; ACEI/ARB = angiotensin-converting enzyme inhibitor/angiotensin receptor blocker; BMI = body mass index; BP = blood pressure; C = Caucasian; CCB = calcium channel blocker; H = Hispanic; ΔPQ = change in mean pulmonary arterial pressure; LVEF = left ventricular ejection fraction; mPAP = mean pulmonary arterial pressure; NT-proBNP = N-terminal pro-B-type natriuretic peptide; PAWP = pulmonary arterial wedge pressure; PH = pulmonary hypertension; PVR = pulmonary vascular resistance; RAP = right atrial pressure; RVEF = right ventricular ejection fraction; VO_2 = oxygen uptake; WU = Wood units.

TABLE 2

Metabolite Levels and Hemodynamic Indexes of RV-PV Function

Metabolite	RAP (Rest)	mPAP (Rest)	PAWP (Rest)	PVR (Rest)	PVR (Exercise)	ΔPQ (Exercise)
Arg/NO metabolism						
Arginine	−0.29 (0.014)	−0.44 (<0.001)	−0.31 (0.007)	−0.31 (0.008)	−0.23 (0.058)	−0.30 (0.013)
Citrulline	−0.12 (0.337)	0.08 (0.515)	0.01 (0.940)	0.21 (0.081)	0.22 (0.069)	0.32 (0.007)
Ornithine	0.014 (0.907)	0.05 (0.682)	0.03 (0.780)	0.02 (0.880)	0.05 (0.703)	0.29 (0.013)
ADMA	0.13 (0.297)	0.12 (0.301)	−0.04 (0.757)	0.16 (0.195)	0.14 (0.233)	0.30 (0.011)
SDMA	0.14 (0.234)	0.27 (0.025)	0.11 (0.373)	0.28 (0.017)	0.36 (0.002)	0.37 (.001)
Arg/(Orn+Citr)	−0.21 (0.074)	−0.44 (<0.001)	−0.29 (0.014)	−0.36 (0.002)	−0.31 (0.009)	−0.53 (<0.001)
Arg/NO score *	0.32 (0.007)	0.44 (0.001)	0.31 (0.019)	0.39 (0.001)	0.32 (0.006)	0.53 (<0.001)
IDO metabolites						
Kynurenine	0.50 (<0.001)	0.46 (<0.001)	0.35 (0.002)	0.30 (0.012)	0.38 (0.001)	0.48 (<0.001)
Anthranilate	0.16 (0.187)	0.39 (0.001)	0.12 (0.302)	0.43 (<0.001)	0.43 (<0.001)	0.49 (<0.001)
Kynurenate	0.17 (0.168)	0.26 (0.032)	0.13 (0.262)	0.29 (0.014)	0.28 (0.02)	0.34 (0.004)
Quinolinate	0.44 (<0.001)	0.43 (<0.001)	0.26 (0.028)	0.32 (0.007)	0.39 (0.001)	0.53 (<0.001)
IDO-TM score *	0.40 (<0.001)	0.46 (<0.001)	0.29 (0.011)	0.41 (<0.001)	0.45 (<0.001)	0.55 (<0.001)
Purine metabolites						
Inosine	0.31 (0.008)	0.28 (0.020)	0.26 (0.027)	0.14 (0.250)	0.16 (0.188)	0.34 (0.004)
Xanthosine	0.28 (0.021)	0.39 (0.001)	0.23 (0.052)	0.27 (0.329)	0.29 (0.051)	0.47 (<0.001)
Xanthine	0.36 (0.002)	0.34 (0.004)	0.24 (0.040)	0.24 (0.044)	0.25 (0.033)	0.40 (0.001)
Uric acid	0.38 (0.001)	0.45 (<0.001)	0.35 (0.003)	0.39 (0.001)	0.33 (0.005)	0.23 (0.054)
Allantoin	0.11 (0.363)	0.25 (0.038)	0.17 (0.165)	0.31 (0.009)	0.26 (0.029)	0.24 (0.043)
Purine score *	0.47 (<0.001)	0.46 (<0.001)	0.53 (<0.001)	0.39 (0.001)	0.36 (0.002)	0.45 (<0.001)
TCA cycle						
Malate	0.27 (0.022)	0.35 (0.002)	0.20 (0.092)	0.39 (0.001)	0.30 (0.011)	0.33 (0.005)
Succinate	0.13 (0.269)	0.39 (0.001)	0.15 (0.202)	0.52 (<0.001)	0.33 (0.005)	0.24 (0.041)
Aconitate	0.15 (0.217)	0.177 (0.162)	0.16 (0.177)	0.34 (0.004)	0.30 (0.013)	0.31 (0.010)
Isocitrate	0.12 (0.335)	0.23 (0.051)	0.16 (0.196)	0.28 (0.017)	0.21 (0.081)	0.16 (0.175)
TCA score *	0.32 (0.007)	0.4 (0.001)	0.22 (0.09)	0.42 (<0.0001)	0.32 (0.006)	0.28 (0.02)
Known biomarker						
NT-proBNP	0.14 (0.261)	0.40 (0.001)	0.40 (0.001)	0.30 (0.013)	0.33 (0.007)	0.38 (0.001)

Values are β-coefficients (p value) and are presented to describe associations between log-transformed metabolite levels and hemodynamic measurements.

* Multimarker scores described in Methods.

ADMA = asymmetric dimethylarginine; Arg/NO = arginine/nitric oxide; IDO-TM = indoleamine 2,3-dioxygenase tryptophan metabolite; Orn+Citr = ornithine plus citrulline; RV-PV = right ventricular-pulmonary vascular; SDMA = symmetric dimethylarginine; TCA = tricarboxylic acid; other abbreviations as in Table 1.

TABLE 3

IDO-TM and Hemodynamic Measurements in Adjusted Models

Metabolite	RAP (Rest)	mPAP (Rest)	PAWP (Rest)	PVR (Rest)	PVR (Exercise)	ΔPQ (Exercise)
Models adjusted for age and sex						
Kynurenine	0.50 (<0.001)	0.44 (<0.001)	0.34 (0.004)	0.28 (0.019)	0.38 (0.002)	0.49 (<0.001)
Anthranilate	0.19 (0.092)	0.34 (0.002)	0.09 (0.414)	0.37 (0.001)	0.36 (0.002)	0.39 (0.001)
Kynurenate	0.36 (0.002)	0.20 (0.078)	0.10 (0.387)	0.24 (0.037)	0.21 (0.069)	0.25 (0.038)
Quinolinate	0.45 (<0.001)	0.39 (0.001)	0.23 (0.045)	0.28 (0.017)	0.36 (0.002)	0.50 (<0.001)
IDO-TM score	0.46 (0.001)	0.42 (<0.001)	0.27 (0.019)	0.35 (0.002)	0.40 (<0.001)	0.50 (<0.001)
Models adjusted for age, sex, and log cystatin C						
Kynurenine	0.01 (0.900)	0.01 (0.995)	0.06 (0.592)	0.12 (0.264)	0.06 (0.598)	0.07 (0.581)
Anthranilate	0.02 (0.803)	0.19 (0.093)	0.05 (0.655)	0.27 (0.009)	0.23 (0.032)	0.24 (0.037)
Kynurenate	0.33 (0.002)	0.23 (0.039)	0.17 (0.116)	0.13 (0.217)	0.20 (0.067)	0.30 (0.011)
Quinolinate	0.23 (0.018)	0.13 (0.184)	0.02 (0.830)	0.11 (0.251)	0.16 (0.12)	0.28 (0.008)
IDO-TM score	0.24 (0.013)	0.19 (0.046)	0.07 (0.479)	0.20 (0.031)	0.20 (0.036)	0.28 (0.007)
Models adjusted for age, sex, and log NT-proBNP						
Kynurenine	0.12 (0.312)	0.12 (0.359)	0.02 (0.895)	0.17 (0.165)	0.14 (0.265)	0.18 (0.190)
Anthranilate	0.13 (0.260)	0.24 (0.043)	0.05 (0.663)	0.30 (0.009)	0.27 (0.022)	0.30 (0.016)
Kynurenate	0.45 (<0.001)	0.35 (0.008)	0.24 (0.070)	0.19 (0.147)	0.29 (0.027)	0.43 (0.002)
Quinolinate	0.42 (0.001)	0.38 (0.004)	0.16 (0.209)	0.23 (0.074)	0.33 (0.012)	0.50 (<0.001)
IDO-TM score	0.40 (<0.001)	0.34 (0.006)	0.16 (0.219)	0.27 (0.022)	0.32 (0.010)	0.44 (0.001)
Models adjusted for age, sex, and IL-6						
Kynurenine	0.51 (<0.001)	0.37 (0.001)	0.22 (0.129)	0.20 (0.083)	0.27 (0.011)	0.36 (<0.001)
Anthranilate	0.21 (0.139)	0.28 (0.032)	0.06 (0.727)	0.31 (0.016)	0.25 (0.045)	0.27 (0.022)
Kynurenate	0.18 (0.167)	0.16 (0.178)	0.12 (0.398)	0.20 (0.093)	0.15 (0.180)	0.18 (0.10)
Quinolinate	0.49 (<0.001)	0.33 (0.005)	0.13 (0.389)	0.19 (0.104)	0.25 (0.024)	0.38 (<0.001)
IDO-TM score	0.47 (<0.001)	0.37 (0.002)	0.17 (0.279)	0.28 (0.024)	0.30 (0.011)	0.39 (<0.001)
Stepwise regression models adjusted for age, sex, IL-6, NT-proBNP, cystatin C						
Kynurenine	0.50 (<0.001)	0.33 (0.004)	0.12 (0.200)	0.09 (0.510)	0.27 (0.022)	0.32 (0.003)
Anthranilate	0.03 (0.778)	0.13 (0.294)	0.03 (0.814)	0.34 (0.004)	0.32 (0.007)	0.16 (0.234)
Kynurenate	0.07 (0.633)	0.11 (0.478)	0.06 (0.637)	0.24 (0.038)	0.15 (0.180)	0.08 (0.528)
Quinolinate	0.44 (<0.001)	0.33 (0.005)	0.12 (0.326)	0.06 (0.71)	0.25 (0.027)	0.35 (0.002)
IDO-TM score	0.45 (<0.001)	0.31 (0.010)	0.26 (0.027)	0.31 (0.010)	0.34 (0.005)	0.38 (<0.001)

Values are β-coefficients (p value) and are presented to describe associations between log-transformed metabolite levels and hemodynamic measurements.

IL = interleukin; other abbreviations as in Tables 1 and 2.

TABLE 4

Validation Cohort: Metabolite Levels and RV-PV Function

Pathway	RAP (Rest)	mPAP (Rest)	PAWP (Rest)	PVR (Rest)	PVR (Exercise)	ΔPQ (Exercise)
Arg/NO metabolites	**0.34 (0.004)**	**0.36 (0.003)**	0.26 (0.026)	0.35 (0.014)	0.28 (0.016)	0.22 (0.064)
IDO metabolites	0.28 (0.018)	**0.43 (<0.001)**	0.23 (0.042)	**0.30 (0.010)**	0.28 (0.019)	**0.36 (0.002)**
Purine metabolites	0.14 (0.25)	0.31 (0.013)	0.07 (0.58)	0.21 (0.07)	0.26 (0.027)	0.20 (0.10)
TCA metabolites	0.26 (0.027)	**0.36 (0.003)**	0.17 (0.19)	0.27 (0.024)	**0.32 (0.007)**	0.28 (0.019)

Values are β-coefficients (p values) for regression analyses in the validation cohort relating each metabolic pathway score to hemodynamic measurements. **Bold** indicates metabolites with β-coefficients that achieved statistical significance with $p < 0.0125$.

Abbreviations as in Tables 1 and 2.

TABLE 5

Variables Predicting the Presence of RV-PV Dysfunction

	Model 1		Model 2		Model 3	
	C-Statistic	p Value	C-Statistic	p Value	C-Statistic	p Value
Model without metabolites	0.68		0.72		0.82	
Kynurenine	0.76	0.007	0.80	0.004	0.86	0.03
Quinolinate	0.72	0.05	0.75	0.07	0.85	0.13
Anthranilate	0.71	0.11	0.74	0.10	0.87	0.01
Kynurenate	0.75	0.04	0.79	0.01	0.88	0.02
IDO score	0.74	0.01	0.79	0.006	0.87	0.01

Model 1: Consists of readily available clinical variables associated with pulmonary hypertension (age, sex, body mass index). Model 2: Adds pulmonary artery wedge pressure to model 1 variables. Model 3: Adds measured right ventricular ejection fraction; omits body mass index based on lack of significant association with any of the metabolite levels or pulmonary hypertension.

Abbreviations as in Table 2.

TABLE 6

PAH Validation Cohort Characteristics

	PAH (n = 11)	Controls (n = 19)	p Value
Age, yrs	44.9 ± 19.5	39.1 ± 10.4	0.61
Female	82	75	0.71
BMI, kg/m^2	27.6 ± 6.6	25.6 ± 4.4	0.36
Diabetes mellitus	0 (0)	0 (0)	1.0
Obstructive sleep apnea	1 (9)	0 (0)	0.37
Systemic hypertension	1 (9)	2 (11)	0.70
Liver disease	0 (0)	0 (0)	1.0
Atherosclerosis	1 (9)	0 (0)	0.37
Active cancer	1 (9)	0 (0)	1.0
Medications			
CCB	1 (9)	0 (0)	0.37
Prostacyclin	6 (55)	0 (0)	0.003
ERA	2 (18)	0 (0)	0.13
PDE5i	3 (27)	0 (0)	0.04
RAP (rest), mm Hg	11 ± 77	NA	
mPAP (rest), mm Hg	55 ± 16	NA	
PAWP (rest), mm Hg	11 ± 77	NA	
Cardiac output, l/min	3.9 ± 1.0	NA	
PVR, WU	13.1 ± 4.3	NA	
Anthranilate, AU	5.8 ± 2.7	3.0 ± 0.9e5	0.002
Kynurenate, AU	5.2 ± 2.7e4	4.9 ± 3.0e4	0.71
Kynurenine, AU	1.8 ± 0.7e5	1.2 ± 0.4e5	0.008
Quinolinate, AU	4.4 ± 0.3e5	1.8 ± 0.4e5	0.001

Values are mean ± SD, %, or n (%).

AU = arbitrary unit; ERA = endothelin receptor antagonist; NA = not available; PAH = pulmonary arterial hypertension; PDE5i = phosphodiesterase type 5 inhibitor; other abbreviations as in Table 1.